3. The Italian high-altitude atmospheric observation network

P. Cristofanelli[1], D. Putero[1], L. Naitza[1], A. Marinoni[1], F. Calzolari[1], F. Roccato[1], M. Busetto[1], T. C. Landi[1], M. Mazzola[1], A di Sarra[2], D. Meloni[2], D. Sferlazzo[2], G. Pace[2], S. Piacentino[2], P. Trisolino[1], E. Aruffo[3], P. Di Carlo[3], M. Bencardino[4], F. D'Amore[4], F. Sprovieri[4], N. Pirrone[4], F. Dallo[5], J. Gabrieli[5], M. Vardè[5], C. Barbante[5], M. Maione[6], J. Arduini[6], P. Bonasoni[1]

[1]CNR-ISAC, National Research Council of Italy, Institute of Atmospheric Sciences and Climate, Bologna, Italy
[2]ENEA, Roma, Italy
[3]University "G. d'Annunzio" of Chieti-Pescara, Department of Psychological, Health & Territorial Sciences, Chieti, Italy
[4]National Research Council of Italy, Institute of Atmospheric Pollution, Rende, Italy
[5]National Research Council of Italy, Institute of Dynamics for Environmental Processess, Venezia, Italy
[6]University of Urbino, Department of Pure and Applied Sciences, Urbino, Italy

3.1 Difficulties in measuring the mountain environment

Measurements of atmospheric composition are challenging at remote measurement sites characterized by harsh environmental conditions like mountains: access to stable power supply is often difficult, as well as shipping of materials (instrumentation/consumables) and personnel stay or travel. For what concern "*in-situ*" observations of trace gases and atmospheric aerosol, the air collection systems must be able to guarantee the correct execution of air sampling during ice rimming or windy conditions (typical for high mountain sites) but also to avoid sampling artifact (i.e. loss of aerosol particle by non-laminar flow, hygroscopic growth of aerosol particles, interaction of gas molecules with water droplets, volatilization of trace gases from the aerosol phase). Snow accumulation and ice rimming represent a limitation also for ground-based remote sensing systems (e.g. photometers, DOAS instruments, LiDAR). Logistic and environmental constraints are coupled with the necessity of using enhanced, often "not-conventional", instrumental set-up for detecting and quantifying with enough accuracy atmospheric species that, in some cases, are present in order of magnitudes lower than at the Earth's surface. This is the case, for instance, of reactive or halogenated gases which mole fractions are typically in the range of nmol/mol (i.e. ppb) to pmol/mol (i.e. ppt). Therefore, sophisticated instrumentation and technical devices, often not directly available through the commercial market, are needed to quantify their abundance with low uncertainties. A further critical point for execution of reliable atmospheric composition observations is the maintaining of consistent calibration scales and quality assurance system: some of the reference materials are unstable and need frequent replacement, while calibration events must be automatized where frequent calibrations are needed. Specific materials must be used to avoid artifacts. As stressed by Schultz et al. (2015) for reactive gases, for some atmospheric species, long-term trends are small relative to the atmospheric variability and their detection needs ambitious data quality objectives to be reached besides the ability (not only technical, but also financial) to sustain over long-term such observing programmes. For these reasons, an important activity within NextData was devoted to share

experiences and knowledge among the different atmospheric observatories to increase the possibility of a successful implementation of the measurement programmes.

3.2 The GAW network and the Monte Cimone Observatory

The monitoring of trace atmospheric constituents in the lower troposphere still represents a fundamental activity to assess their long- and short-term variability, to investigate their driving processes and to assess the impact of natural and anthropogenic sources into the atmosphere. The Global Atmosphere Watch program of the World Meteorological Organization (WMO/GAW) coordinates a global network of surface stations to understand and control the increasing influence of human activity on the global atmosphere (WMO, 2017). The backbone of the WMO/GAW is a global network of more than 400 surface stations, performing routine observations of atmospheric constituents in the troposphere/stratosphere. Atmospheric stations belonging to the WMO/GAW network are requested to adopt standard operating procedures (SOP), quality assurance (QA) programs and routinely submit data to perform quality assurance/quality (QA/QC) check actions and routinely submit data to specific World Data Centers (WDCs) covering 6 focal areas (i.e., atmospheric aerosols, greenhouse gases, selected reactive gases, ozone, UV radiation, precipitation chemistry). Among the hundreds of measurement stations, 31 are defined as "global" (at the current date: 2018, July). WMO/GAW global stations must comply with a set of well-defined criteria. Among these: the measurement programme must cover three focal areas at least, the spatial representativeness of the atmospheric measurements must extend over the regional perspective, long-term commitments must be assured by funding and managing agencies, measurement programmes must strictly follow WMO/GAW SOP and be compliant with QA request.

In the Mediterranean region, the only WMO/GAW global station is based at Mt. Cimone (2165 m a.s.l., northern Apennines) and it is composed by the CNR "O. Vittori" observatory and by the meteorological observatory of the Italian Air Force. Both these research infrastructures are located above the timberline and only some patches of grass can be found on the mountaintop, which is mostly rocky and covered with snow for 6-7 months a year. In spring, the last snowfall generally takes place in mid-April while in autumn the early snowfall usually occurs in mid-November.

Mt. Cimone is the windiest meteorological station in Italy (wind speed higher than 200 km/h are occasionally observed) and the prevailing winds blow from S-SW and N-NE (Colombo et al., 2000). As deduced by the "O. Vittori" observatory measurements, the lowest monthly mean temperature was in February 2005 (-7.9°C), and the highest in July 2015 (14.9°C) over the period 1996 - 2017. The annual mean (as deduced by averaging monthly mean values) is 2.1 °C. As reported by previous investigations, the atmospheric observations carried out at CMN can be considered representative of the free tropospheric conditions of the Mediterranean basin / South Europe during the cold months (see e.g. Bonasoni et al., 2000; Henne et al., 2010) as well as during night-time in the warm season. However, from April to September, the measurement site can be affected by "thermal" wind circulation and convective vertical transport of air masses. Indeed, as also pointed out by a study carried out in the framework of NextData (Cristofanelli et al., 2015) during day-time, up-slope and valley winds together with diurnal planetary boundary layer (PBL)

growth and entrainment processes, can favor the vertical transport of polluted PBL air to the measurement site.

The CNR "O. Vittori" observatory offers the possibility to access an advanced research infrastructure to investigate the processes affecting atmospheric background composition. The station is completely automated and no scientific personnel is permanently working at the site. It is composed by the "reactive gas" laboratory (equipped with a sampling system optimized for reactive and greenhouse gases), the "aerosol" laboratory (equipped with a sampling system optimized for aerosol particles) and the "greenhouse gas" laboratory, where instrumentation from Urbino University for halogenated gases (CFCs, HCFCs, HFCs), volatile anthropogenic organic compounds, methane, SF6 are hosted. The air intakes for trace gas and aerosol particles allow continuous air-sampling even during extreme weather conditions (high wind speed conditions and ice rimming, see Cristofanelli et al., 2017).

Two high volume samplers for PM10 and PM10/PM1 are accommodate in a specific designed shelter on the observatory terrace: they are used for aerosol chemistry characterization during specific experiments and field campaign (e.g. Decesari et al., 2017). The terrace (about 40 m^2) is equipped for hosting external experimental activity (e.g. solar photometry). A fast internet connection is available thanks to the Emilia-Romagna Region throughout Lepida S.p.A.. This high-speed internet connection allows the remote control of instrumentation as well as near-real time (NRT) data delivery which is a pre-requisite for the implementation of science services devoted to data sharing/validation (see Section 4.3.2) and early warning (see Section 4.3.4). A dedicated web page reports the last 24 hours of on-line observations (www.isac.cnr.it/cimone/real-time).

Thanks to the implementation activities carried out within NextData, the experimental set-up at the CNR observatory was implemented with a Cavity Ring Down System instrument for the simultaneous observations of CO_2, CH_4 and CO. This was a fundamental step for the beginning of the labelling processes within the ICOS (Integrated Carbon Observation System) Research Infrastructure (Hazan et al., 2016). NextData also favored the implementation of NO_x (NO and NO_2) measurements at the "O. Vittori" observatory with a Chemioluminescence detection (CLD) instrument equipped with a photolytic "blue light" converter for conversion of NO_2 to NO (Steinbacher et al., 2007). Together with the implementation of a system specifically designed for the execution of automatic calibrations, this allowed the "O. Vittori" observatory to be included in the reactive gases component of the ACTRIS-2 H2020 project, which is propaedeutic to the implementation of ACTRIS (Aerosol, Clouds, Trace gases Research Infrastructure). In this regards, NextData also supported the implementation of the "near-surface" aerosol components by the implementation of back-scattering (Muller et al., 2011) and sub-micrometric size distribution observations (Wiedensohler et al., 2012).

3.3 Italian high-altitude atmospheric composition network

In Italy, the NextData project was aimed at favoring the integration of a network in mountain and remote areas, based on atmospheric observatories for the monitoring of atmospheric composition and ancillary data (meteorological parameters and solar radiation). The main goal of this network is to investigate the processes, which influence the variability of air pollutants and climate-altering

compounds to contribute towards a better assessment of related impacts to mountain ecosystems and climate in the Mediterranean basin. The network comprises five high-mountain atmospheric observatories (Fig. 1): Monte Cimone (CMN, northern Apennines, the only WMO/GAW global station in Italy; 2165 m a.s.l.), Plateau Rosa (PRS, western Alps, WMO/GAW regional station; 3480 m a.s.l.), Col Margherita (MRG, eastern Alps; 2550 m a.s.l.), Monte Portella – Campo Imperatore (CMP, central Apennines; 2401 m a.s.l.), and Monte Curcio (CUR, southern Apennines, WMO/GAW regional station; 1796 m a.s.l.). In addition to these observatories, the WMO/GAW regional stations Capo Granitola (CGR, south-western Sicily) and Lampedusa (LMP, central Mediterranean Sea), provide complementary information on the background conditions of the Mediterranean basin marine boundary layer.

Six of these observatories are already part of international projects/research programmes for the monitoring of Essential Climate Variables (ECVs). More specifically, in the framework of the WMO/GAW activities, observations of greenhouse and reactive gases are carried out at Plateau Rosa, Mt. Cimone, Mt. Curcio, Capo Granitola and Lampedusa (Table 1). Moreover, Plateau Rosa, Mt. Cimone and Lampedusa also started the labelling processes to be included in the European Research Infrastructure ICOS (Integrated Carbon Observation System, http://www.icos-ri.eu, see Hazan et al., 2016). Measurements of physical properties of atmospheric aerosols are performed at Mt. Cimone, Mt. Curcio, and Capo Granitola. Mt. Cimone is part of ACTRIS-2 (Aerosols, Clouds and Trace gases Research Infrastructure, https://www.actris.eu/, see FMI 2017) which aims in consolidating high-quality observations of aerosols, clouds and trace gases. Col Margherita and Mt. Curcio are part of GMOS (Global Mercury Observation System), a global observational network providing comparable data on mercury levels in ambient air and deposition (see Cinnirella et al., 2014; Sprovieri et al., 2016). Within GMOS a web-based system for QA/QC has been developed in order to check raw data related to atmospheric mercury (D'Amore et al. 2015).

The observational network for monitoring the background environmental-climatic conditions aims to contribute at international projects and programmes: e.g. GAW-WMO, ACTRIS and ICOS-RI. The first goal of the NextData Project is to contribute, during its activity period, in supporting the operation of the atmospheric background stations. This will be accomplished by strengthening the observation and technical equipment, by sharing and disseminating standard methodology and SOPs for the observed ECVs, by implementing common automatic systems for the quality assurance/check (QA/QC) and for the data reporting.

Figure 1. *Geographical location and pictures of the monitoring stations considered in this work.*

ECV	Reference programmes	Monitoring stations						
		PRS	MRG	CMN	CMP	CUR	CGR	LMP
CO_2	WMO/GAW ICOS	X		X		X	X	X
CH_4		X		X		X	X	X
CO		X		X		X	X	X
O_3			X	X	X	X	X	X
SO_2				X		X	X	
NO	WMO/GAW ACTRIS			X		X	X	
NO_2				X		X	X	
Particle scattering				X		X	X	
Particle absorption				X		X	X	
Particle size distribution (by SMPS)				X		X		
Particle concentration				X		X	X	
Coarse particle size distribution (by OPC)				X	X	X	X	
AOD[1]				X				X
Meteorological parameters	WMO/GAW	X	X	X	X	X	X	X
Solar radiation			X	X	X	X	X	X

Table 1. *List of Essential Climate Variables (ECVs) collected at the atmospheric background monitoring observatories. Grey-shaded cells indicate the ECVs included in the automatic processing chains. [1]AOD measurements are processed in the framework of AERONET and GAW-NRT programs.*

3.3.1 Definition of guidelines to harmonize the measurement methodologies, protocols, QA/QC procedures, including the adoption of common reference calibration scales (e.g. GAW-WMO, ICOS, ACTRIS)

To contribute in facilitating and strengthening the Italian contribution to international projects and programmes concerning the investigation of atmospheric composition changes (e.g. WMO/GAW, ACTRIS-RI, ICOS-RI), for each observed ECV, NextData favoured the adoption of measurement guidelines and SOP defined by the reference international programmes (Table 3). These information have been shared within the NextData community and specific efforts have been carried out to implement common measurement standards linked to international reference scales (Table 3). For instance, for near-surface O_3 observations, carried out at MRG, CMN, CMP, CUR, LMP and CRG have been related to the WMO SRP#15 scale by using a secondary O_3 photometer hosted at CNR-ISAC laboratory in Bologna. WMO reference scale has been implemented at CMN and CGR for NO by adoption of standard by the National Physical Laboratory (UK) - NPL (WMO, 2017), as well as for CO, CH_4 and SF_6 at CMN by a set of secondary standard from the National Ocean and Atmospheric Administration - Earth System Research Laboratory (NOAA – ESRL). At this station, for CO_2, CH_4 and CO also the ICOS calibration scales, which are linked with WMO calibration scales, have been implemented by the adoption of calibration standard produced by the ICOS Calibration Laboratory (Hazan et al., 2016). The WMO calibration scales for CO_2, CH_4 and CO have been propagated at CGR by means of references cylinders from CMN and LMP.

ECV	Reference programmes	Guidelines/SOP	Calibration Center
Near-surface ozone	WMO/GAW	GAW Report No. 209,	NOAA-ESRL/EMPA
NO, NO_2	WMO/GAW	GAW Report No. 209, GAW Report No. 232	NPL
SO_2	WMO/GAW	-	-
CO	WMO/GAW – ICOS	GAW Report No. 192	NOAA-ESRL/EMPA
CO_2	WMO/GAW – ICOS	GAW Report No. 213.	NOAA-ESRL/MPI-Jena[1]
CH_4	WMO/GAW – ICOS	GAW Report No. 213.	NOAA-ESRL/MPI-Jena[1]
N_2O	WMO/GAW – ICOS	GAW Report No. 213.	NOAA-ESRL/MPI-Jena[1]
SF_6	WMO/GAW	GAW Report No. 213.	NOAA-ESRL
Aerosol light absorption/scattering	WMO/GAW – ACTRIS	GAW Report No. 200 Anderson et al., 1998:Petzold et al., 2004	WCCAP-TROPOS (ACTRIS/WMO)
Particle size distribution	WMO/GAW - ACTRIS	GAW Report No. 227 Wiedensohler et al., 2012	WCCAP-TROPOS (ACTRIS/WMO)
Particle number concentration	WMO/GAW – ACTRIS	GAW Report No. 227	WCCAP-TROPOS (ACTRIS/WMO)
Aerosol Optical Depth	WMO/GAW	GAW Report No. 227	PMOD/WRC

***Table 3**. List of reference programmes, guidelines and SOP documents, calibration center for each ECV.*
[1]Within ICOS

3.3.2 Automatic procedures for submitting essential climate variables (ECVs) recorded at Italian Atmospheric Observatories to WMO/GAW data centres

In the framework of the National Project of Interest NextData, we developed a set of procedures for the automatic flagging and formatting of different ECVs to be submitted to the World Data Centres (WDCs) of the WMO/GAW. The NextData system does not generate "consolidated" data to be directly submitted to WDCs, but it represents a valuable tool to facilitate data providers towards a more efficient data production streams. Our procedures are expected to accelerate the process of data submission to GAW/WMO or to other reference data centres or repositories as well as to make the data flagging more "objective". This implies the adoption of a suite of well-defined flagging criteria not strictly related to the subjective judgment of station operators. Finally, it must be clearly stated that this action would not overcome the quality assurance/quality check activity carried out at the topical/thematic centres of integrated initiatives (e.g., ICOS, ACTRIS), nor at WMO/GAW WDCs.

Besides making the data creation process faster, it also promotes a timely data submission, and the adoption of standardized flagging procedures will also assure a more subjective data verification, as well as the possibility to trace back the actions which led to data validation (i.e., data revisions will be easier).

Currently, the automatic processing of ECV data is active for a subset of NextData measurement sites (MRG, CMN, LMP, CGR, CMP) which agreed in participating to this activity. In particular, the Mt. Cimone WMO/GAW global station was selected as a "proof-of-concept site", due to the large number of ECVs observed and the large variety of data formats produced by the different measurement systems implemented during more than 20 years of scientific activity. Specific procedures have been developed for each ECV and for each instrument used by the considered stations: Table 4 summarizes the list of these instruments, together with the formats used for data file creation. All the procedures have been implemented in "R" Language and Environment for Statistical Computing (R Core Team, 2015). It is important to note that these routines, even if implemented for a specific suite of devices, can be virtually adapted to other instruments using the same principle of operation/detection.

The automatic processing encompasses a preliminary harmonization of file formats, which is the pre-requisite for the subsequent data flagging, data aggregation (to common temporal frames: 1 and 60 minutes), and final format harmonization. The greenhouse gases (CO_2, CH_4) and the carbon monoxide (CO) files are created in agreement with formats and metadata indicated by the WDCGG, as reported in "Revision of the WDCGG Data Submission and Dissemination Guide" (GAW Report No. 188). "Near-surface" reactive gases, aerosol properties and meteorological parameters are formatted following the NASA-Ames standard, as indicated by WMO/GAW WDCRG and WDCA. This format is based on the textual format ASCII NASA-Ames 1001 with additional metadata (as a function of the different ECVs). The file templates to be used for each ECV can be found at the web page http://ebas-submit.nilu.no/Submit-Data/Reporting-Templates/all-templates-temporary. The files created by the automatic processing chain contain all of the observations carried out during a full solar year; they are updated on a daily basis.

Class	ECV	Instruments	Data file format
Trace gases (near-surface)	Ozone	Thermo 49i, Thermo 49c	NASA-AMES
	NO, NO_2	Thermo 42iTL	NASA-AMES
	SO_2	Thermo 43iTL	NASA-AMES
	*CO	Picarro G2401	Ascii (WDCGG)
	*CO_2, CH_4	Picarro G2401	Ascii (WDCGG)
Aerosol (near-surface)	Aborption coefficient	MAAP 5012	NASA-AMES
	Aerosol scattering	TSI 3563	NASA-AMES
	Number particle concentration	TSI 3775	NASA-AMES
	Size distribution	OPS (Grimm 1.108)	NASA-AMES
Meteorology	T, RH, P, WD, WS Global	Various	NASA-AMES

Table 4. *Summary of automated procedures developed for the processing of ECVs as a function of specific instruments and data file format for submission to WMO/GAW WDCs.* Automatic processing still not operative. For explanation of "data file formats" see Section 3.3.4*

To increase the inter-operability of the automatic procedures, the sequential steps of the workflow are the same for all the different ECVs:

1) data collection of raw files;
2) data formatting of raw files;
3) data check and flagging;
4) data correction (if needed);
5) data aggregation (time averaging) and flagging;
6) data formatting;
7) creation of data reports.

With this process in 7 steps, three different data levels are produced according with WMO/GAW WCDRG and WCDA data reporting guidelines (see also https://ebas-submit.nilu.no/Submit-Data/Data-Reporting):

- Level-0: annotated raw data; format instrument specific; contains all parameters provided by the instrument; contains all parameters/info needed for processing to final value; "native" time resolution;
- Level-1: data processed to final parameter (calibration and correction implemented to data series), invalid data and calibration episodes removed, "native" time resolution, correction to standard temperature and pressure (i.e., 273.15 K, 1013.25 hPa);
- Level-2: data aggregated to hourly averages, atmospheric variability quantified by standard deviation or percentiles.

The instrumental raw data are transferred (at least) once a day from the measurement stations to a server located at CNR-ISAC HQs in Bologna. The files stored at the CNR-ISAC server already

contain information of the measured quantities in geophysical units, as well as internal diagnostic parameters used for automatic QA/QC.

The data inspection consists in a series of checks that are automatically performed on data with native time resolution (usually 1-min), with the aim of referring each data record to a set of codified flags (which indicate whether a measurement is valid or not).

The first step of the automatic data check consists in the identification of the different measurement modes: “sample” (when ambient air is measured), “calibration” (when air from one or more laboratory standards is measured), “zero” (when a gas mixture scrubbed by the molecules to be quantified is measured, typically to determine the instrumental zero off-set for routine quality checks) and “span” (when dry air enriched by a specific amount of the molecules to be quantified is measured, typically to point out changes in the instrumental sensitivity).

The identification of the measurement mode, which leads to the attribution of a specific flag to the concurrent data record, is fundamental for two reasons: (1) data affected by calibrations or quality checks must be discarded during time averaging processes, and (2) data recorded during calibrations or quality checks are used to obtain correction factors or quality control metrics.

The measurement periods affected by “calibrations” or “zero/span” checks are selected considering two general cases: (1) by analyzing the variability of internal diagnostic parameters from instrument analyzers or from “calibration units” (e.g., some devices provide the information related to their current measurement mode to the acquisition system), or (2) by searching the existence of a log-file that indicates the start and end times of QC exercises.

The second step is the analysis of the variability of instrumental data (both related to internal diagnostic parameters and to the measured ECV). Such step is based on general criteria, but, at the same time, it is adapted as a function of specific measurement stations and ECVs. The following checks are implemented in the data control process:

- *Diagnostic/instrumental checks*: the internal diagnostic parameters (e.g., temperatures, flows, pressures) are compared with their typical ranges, which are reported on the instrument manuals. For each measurement, if at least one parameter fails a check, the data is flagged as invalid (see e.g., Table 6 for NO and NO_2 threshold values at CMN).
- *Plausibility checks*: the measurement periods with values exceeding the expected variability are selected and identified as “outliers”. The allowed variability ranges are defined as a function of the measurement stations (e.g., the plausible range for atmospheric pressure at a surface station like CGR is different from that of a mountain station like MRG). Currently, two different processes for the definition of these ranges are considered. The first is the adoption of fixed threshold values, defined upon existing literature, and in collaboration with scientists in charge of the instruments. The second process is related to the on-line calculation of variable threshold values basing on statistical data analysis over specific time periods (1 hour, 1 day, 1 month, or a full year), e.g., percentiles of the data-set or confidence intervals like n-times the standard deviation above or below the average values. In this context, different calculations were implemented to detect outliers, and applied to raw data with a valid numflag (no calibration, no sampling failures/interruptions). Following an approach similar to Huang et al. (2016), for a sub-set of aerosol ECVs (number concentration, scattering coefficient, absorption coefficient) outliers are identified (and flagged) if:

$$|x_i - RM_i| \geq n\, RSD_i$$

where x_i is the i^{th} measurement, RM_i and RSD_i are the running mean and running standard deviation for the i^{th} record on a user-defined window (e.g., 3 days), and *n* is a user-defined value to be set according to the instrument and type of the station. For CO_2, CH_4 and CO, the methodology presented in Hazan et al. (2016) and based on the calculation of the standard deviation of a "subset" of representative data to detected "background" measurements, have been implemented.

- *Variability checks*: verification of the variability (i.e., rate of change with respect to time) of the observed ECV. Depending on the considered ECV and the characteristics of each site, a range for minimum and maximum ECV variability is defined (typically on hourly basis)

To support measurement stations in carrying out the QA/QC checks, a suite of graphical reports (i.e., data plots) is produced by the automatic data processing chain. The data reports are updated on a daily basis, by using specific routines. To this aim, some specific functions of the "OpenAir" package (Carslaw and Ropkins, 2012) are also used. A special suite of data reports (the "calendar" or "timevariation" products) were implemented for quick data dissemination towards stakeholders or citizens.

The data reports are arranged as a function of different time windows: daily, monthly, seasonal and yearly. In total, 9 data reports are operationally produced for each ECV (Table 7).

Class	**Description**
GRAPH	Time series
TIMEVARIATION	Daily and weekly average /seasonal cycles
CALENDAR	Daily ECV average value laid out in a calendar format

Table 5. *Description of data reports.*

3.3.3 Access to historical data: MOVIDA-Multistation

To provide open and free access to the historical time series of ECVs recorded at the background stations before NextData, the system MOVIDA-Multistat (http://shiny.bo.isac.cnr.it:3838/plot-multistats-en/) was implemented as an improvement of the system MOVIDA (MonteCimone On-line VIsualization and Data Analyses) realized in collaboration with Arpa Emilia-Romagna (SIMC), under the Common Creative License 3.0. External users can access and download time series (with hourly time resolution) of meteorological parameters (air temperature, relative humidity, atmospheric pressure, wind speed and direction), trace gases (O_3, CO, NO, NO_2, SO_2, CH_4, N_2O, SF_6, HFC134a, CFC-11, CFC-114) and aerosol properties (fine and coarse size distribution, absorption coefficient) recorded at the NextData stations. Moreover, MOVIDA-Multistat represents a web resource by which external users can run some basic statistical analyses on time series for each presented parameter and over flexible period of interest. Thanks to the packages Shiny

(shiny.rstudio.com) and Openair (Carslaw and Ropkins, 2012), it is possible to plot raw data, average (on different time scales: daily, monthly and yearly) as well as to perform smoothing of time series to obtain information about long-term tendencies.

Figure 2. *Web interface of MOVIDA system, available at the web page* http://www.nextdataproject.it/?q=it/content/movida-multistations

3.3.4 Example of application: implementation of NRT data delivery and early warning services

Implementation of an experimental service for detection of dust events

An "early-warning" system for the identification of Saharan dust events (hereinafter SDEs) was implemented at CMN. The system was based on the methodology presented by Duchi et al. (2016), which coupled the observation of in-situ "near-surface" coarse aerosol particle number concentration (in the range Dp = 1–10 µm, obtained by an Optical Particle Counter 1.108 GRIMM) with 3D back-trajectories. More specifically, a "dusty day" was identified when a significant increase in the coarse concentration daily average value was associated with the presence of air-masses originated from northern Africa.

To implement a "near-real time" detection of SDEs at Mt. Cimone, we coupled the detection of increases in the "near-surface" coarse particles number concentration with information of air-mass origin and path, as deduced by back-trajectory forecasts calculated by the Hybrid Single-Particle Lagrangian Integrated Trajectory model (HYSPLIT), see Figure 3. HYSPLIT is developed by NOAA's Air Resources Laboratory, one of the most widely used models for atmospheric trajectory calculations (Stein and Ngan, 2015). On each calendar day, an ensemble of forecasted 120-hour long back-trajectories is calculated for Mt. Cimone, for the next 4th calendar day (see http://www.isac.cnr.it/cimone/hysplit). Back-trajectory calculations are based on the operational NOAA GFSG forecast data file.

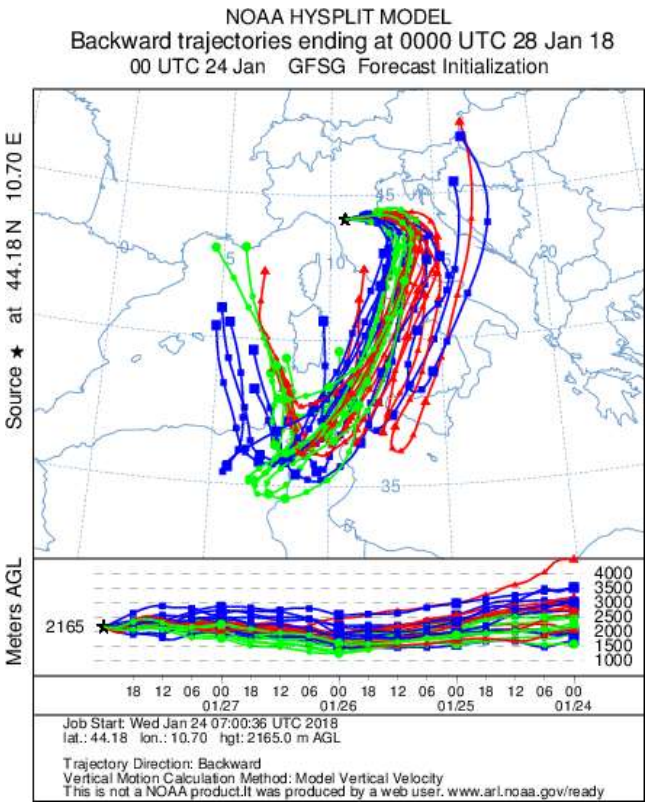

Figure 3. *Example of 120-hour back-trajectory ensemble forecast calculated for CMN by HYSPLIT model. The ensemble describing the air-mass origin for 28th January 2018 at 00:00 UTC was calculated on 24th January 2018 at 00:00 UTC.*

The daily back-trajectory ensemble file is automatically processed to point out the possible passage over a geographical box roughly representing northern Africa. If air-masses are forecasted to pass over northern Africa and an increase of coarse particle concentration is observed for at least three hours (to retain only robust events), a warning is launched by automatic e-mails to a pre-compiled mailing list.

To evaluate the "robustness" of the Saharan dust event detection based on the analysis of the "near-surface" coarse particle number concentration, the aforementioned methodology was compared to another well-known methodology used to assess the occurrence of SDEs at the mountain site Jungfraujoch in the Swiss Alps (Collaud Coen et al., 2004). This reference methodology is based on the simultaneous measurements of scattering and absorption coefficients at different wavelengths, and on the calculation of the wavelength dependence of the single scattering albedo (SSA). The "core" of this methodology is the variation of the Ångström exponent of the single scattering albedo with wavelength (hereafter referred to as α_{SSA}): the authors indicate as SDEs the time periods with negative α_{SSA} for more than 3 hours. This is also visible from the inversion of the wavelength dependence of the SSA during hours characterized by dust transport. At CMN, a three-wavelength integrating nephelometer (TSI 3563) is running since 2014, while a 7-wavelength aethalometer (Magee Scientific AE31) was used to carry out measurements over the period 2011–2015. An application of the Collaud Coen et al. (2004) methodology to Mt. Cimone measurements is shown in Figure 4. To obtain the time series (over the two-year period common to both of the instruments) of the α_{SSA}, we proceeded as follows:

- Scattering coefficients from the nephelometer (λ = 450, 550, and 700 nm) were fitted with a power-law dependence, to determine the scattering exponent α_{sca}
- By using the α_{sca} value, scattering coefficients at the seven wavelengths of the aethalometer (λ = 370, 470, 520, 590, 660, 880, and 950 nm) were then computed
- For each of these 7 wavelengths, the single scattering albedo (SSA) was evaluated, according to $SSA = \frac{\sigma_{sca}}{\sigma_{sca}+\sigma_{abs}}$, where σ_{sca} and σ_{abs} are the scattering and absorption coefficients, respectively
- The seven SSA values were then fitted with a power-law dependence, to obtain α_{SSA}

According to the Collaud Coen et al. (2004) methodology, a total of 107 days characterized by dust transport were observed at Mt. Cimone, for 2014–2015. A sensitivity study was also performed, by varying the minimum consecutive hours to be selected as SDE (i.e., we used either 2 or 4 h), giving no significant differences.

To assess the comparison between the two methodologies, the "dichotomous" approach presented in Thornes and Stephenson (2001) was followed. More specifically, 2×2 contingency tables were computed (Table 6); in these tables, each entry encloses a list of SDE or no-SDE days, defined by the two different methodologies. For a complete explanation of the parameters hereby used, please refer to Thornes and Stephenson (2001) and Wilks (2006). In all of the three comparisons considered (i.e., by using a threshold of 2, 3 and 4 h for the Collaud Coen et al. (2004) methodology), the values of the statistical parameters were similar: the accuracy in the range 0.75–0.78 seems to be in line with what reported in Collaud Coen et al. (2004), i.e., that 71% of SDE cases identified by a negative α_{SSA} are "confirmed" by the presence of trajectories originated in northern Africa. In addition to these parameters, we considered the Odds Ratio Skill Score (ORSS, see Thornes and Stephenson, 2001), a parameter which varies between −1 and +1, where a score of 1 represents perfect skill and a score of 0 indicates no skill. In all cases, the ORSS was above the minimum ORSS required to have skill at the 99% confidence level, thus indicating that the agreement between the two methodologies is statistically significant.

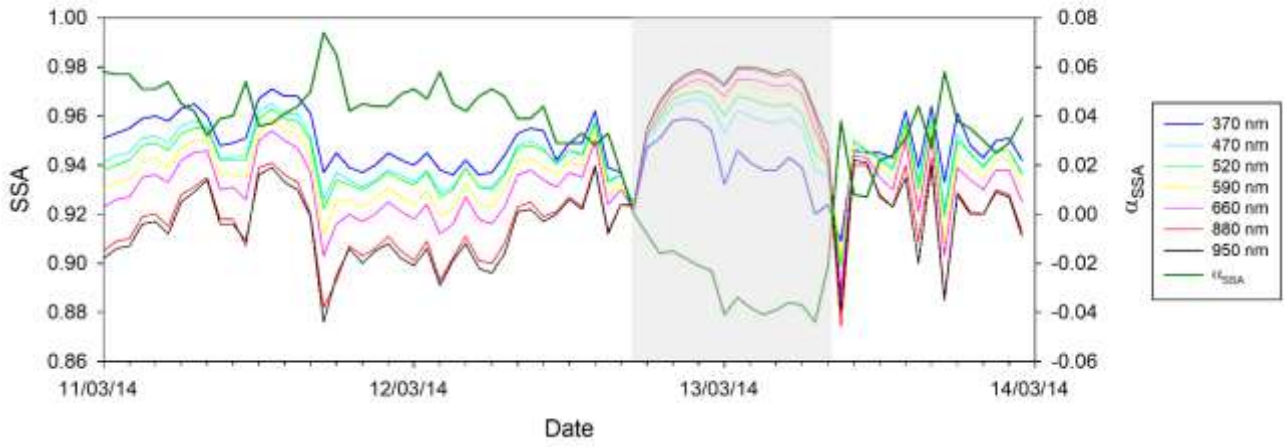

Figure 4. *Temporal evolution (hourly averages) of the calculated single scattering albedo (SSA) during a SDE (shaded area) at CMN, from March 11th to 13th, 2014. Also reported in the plot is the temporal evolution of α_{SSA}, computed by a power-law fit of the SSA values at the seven wavelengths.*

		Duchi et al. (2016)				Duchi et al. (2016)				Duchi et al. (2016)	
		Y	N			Y	N			Y	N
CC (3 h thresh.)	Y	A = 25	B = 73	CC (2h thresh)	Y	A = 33	B = 101	CC (4 h thresh)	Y	A = 23	B = 57
	N	C = 43	D = 324		N	C = 35	D = 296		N	C = 45	D = 340
Accuracy (ACC)		0.75				0.71				0.78	
ORSS		0.44				0.47				0.51	
min ORSS		0.35				0.35				0.35	

Table 6. *The 2×2 contingency tables for the comparison of the DTE event time series, i.e., identified by the Duchi et al. (2016) and the Collaud Coen et al. (2004) – hereby indicated as "CC" – methodologies. For CC, several thresholds on the minimum number of consecutive hours to identify a SDE were chosen (i.e., 2, 3, and 4 h). Capital letters are defined as follows: A indicates the number of SDE days selected by both methodologies, B represents the number of days selected as SDE by the first methodology (Y) but as no-SDE (N) by the second one, C represents the number of days selected as no-SDE by the first methodology but as SDE by the second one, and D represents the number of no-SDE days selected by both methodologies. The table also shows several skill scores, as defined in Thornes and Stephenson (2001), and Wilks (2006).*

Application of STEFLUX to NextData mountain sites

STEFLUX (Stratosphere-to-Troposphere Exchange Flux, see Putero et al., 2016) is a fast-computing tool for the identification of stratospheric intrusion (SI) occurring at a specific location and during a specific time window, developed in the framework of NextData. Its calculations are based on a compiled stratosphere-to-troposphere exchange (STE) climatology (Škerlak et al., 2014), which makes use of the ERA-Interim reanalysis dataset from the ECMWF, as well as a refined version of a well-established Lagrangian methodology. The STE climatology is available from 1979 and continuously updated, allowing also the climatological characterization of SI events for the chosen site.

To assess the STEFLUX ability to routinely identify the occurrence of stratospheric intrusion events at the high-altitude stations of the background network, we carried out a preliminary comparison of STEFLUX outputs and observations at PRS, CMP, and CUR. The time periods of study differed according to the availability of atmospheric measurements at the stations: we chose 2006–2016 for PRS (a), 2012–2016 for CMP (b) and 2015 for CUR (c). The comparison with CMN observations was successfully carried out in the NextData paper by Putero et al. (2016).

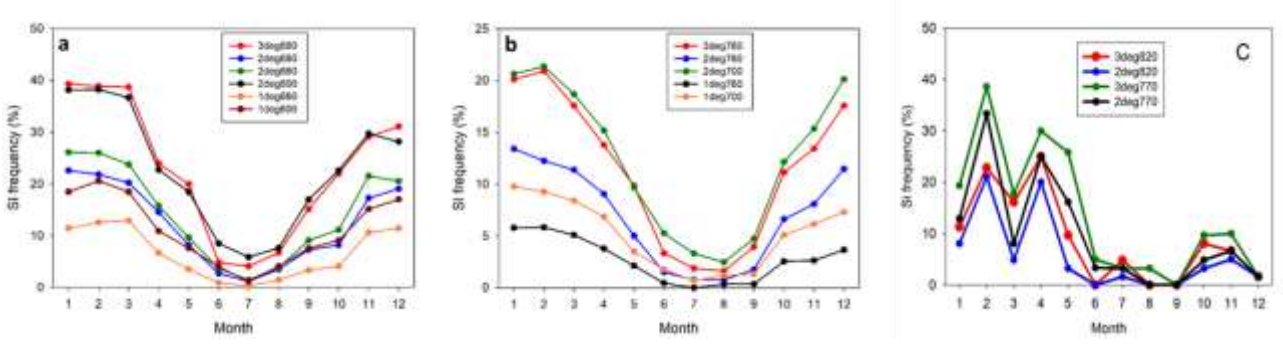

Figure 5. *Annual average variation of SI frequency at PRS (panel a), CMP (b) and CUR (c). Displayed are different configurations for the input parameters of STEFLUX, in the following form: 3deg660 indicates that the "target box" has a horizontal extension of 3°×3° around the measurement site (located as center), and a vertical top lid of 660 hPa.*

STEFLUX was applied at these measurement sites, by selecting different configurations for the input parameters. As input, STEFLUX requires the coordinates of the "target box" (i.e., a geographical area including the measurement site) to be specified, together with its top lid. We specified several "target boxes" centered at the station locations but with different horizontal (from 1° x 1° to 3° x 3°) and vertical boundaries. The results are displayed in Figure 5, where the annual variation of SI frequency, according to different settings, is presented. Please note that CUR presents a more noisy behavior due to the relatively short time period considered. For all the measurement sites, a clear seasonal cycle for SI frequency is discernible with highest values during winter-spring and minima during summer.

The differences between the different configurations are minimized from June to September for all the measurement sites, while the seasonal cycle is larger for the simulations characterized by the "target box" with the highest top lid or the widest horizontal boundaries. In some way, it looks that the definition of the "target box" top lid and horizontal extension can compensate each other: increasing the top lid or increasing the horizontal extension lead to similar result on SI frequency variations.

To assess the STEFLUX performance in identifying period affected by SI at the NextData mountain stations, relative humidity (RH) and ozone (O_3) observations (hourly mean values) were used to objectively identify SI events. According to Cui et al. (2009), if O_3 values are continuously higher than the 10-day running mean by 10% and RH values are below 50% for a time period of at least 6 hours, SI events are identified by measurements (hereinafter "Cui2009_RH+O3"). Because a large fraction of days is characterized by the lack of simultaneous O_3 and RH measurements at the sites, we also considered two less strict identification criteria, which only consider the RH ("Cui2009_RH") or the O_3 ("Cui2009_O3"). Even if this approach does not consider other well-known stratospheric tracers (e.g., ^{7}Be, or potential vorticity), its use in mountain sites is justified by Trickl et al. (2010).

According to STEFLUX, depending on the "target box" configuration, SI events were observed for 19-32% of time for PRS, 9-17% for CMP and 4-12% for CUR, on a yearly basis. On the other side, according to the experimental selection, SI events were identified for 11-49% of time at PRS (for "Cui2009_RH+O3" and "Cui2009_RH", respectively), 24% of time for CMP ("Cui2009_O3"), 7-48% for CUR.

In agreement with Cui et al. (2009) and Putero et al. (2016), a quantitative assessment of STEFLUX performance was accomplished by using the following approach: if during the period of a measured SI event at least one SI event is identified by the model simulation, we consider that STEFLUX well captures the measured SI event. As reported by Tables 7-9, the STEFLUX performance is decreasing with decreasing latitude and height of the measurement sites.

Selection	Days	Cui2009_RH	Cui2009_RH+O3
SF_2deg_680hPa	331 (18.8%)	166 (50.1%)	28 (8.4%)
SF_2deg_660hPa	388 (22.0%)	196 (50.5%)	37 (9.5%)
SF_3deg_660hPa	572 (32.4 %)	278 (48.7%)	57 (10.0%)

Table 7. *Agreement (in number of days and in percentage) between measured SI events at PRS (based on different selection criteria) and STEFLUX outputs for different "target box" top lid (680 hPa and 660 hPa) and horizontal extensions (2°x2° and 3°x3°).*

Selection	Days	Cui2009_RH
SF_2deg_760hPa	15 (8.9%)	4 (27%)
SF_3deg_760hPa	21 (12.6 %)	6 (29%)
SF_2deg_700hPa	29 (17.4%)	10 (24%)

Table 8. *Agreement (in number of days and in percentage) between measured SI events at CMP (based on different selection criteria) and STEFLUX outputs for different "target box" top lid (760 hPa and 700 hPa) and horizontal extensions (2°x2° and 3°x3°).*

Selection	Days	Cui2009_RH	Cui2009_RH+O3
SF_2deg_820hPa	13 (4.1%)	5 (38%)	1 (7%)
SF_3deg_820hPa	22 (6.9 %)	8 (36%)	2 (9%)
SF_2deg_770hPa	28 (7.4%)	9 (32%)	1 (3%)
SF_3deg_770hPa	42 (12.0 %)	15 (36%)	2 (5%)

Table 9. *Agreement (in number of days and in percentage) between measured SI events at CUR (based on different selection criteria) and STEFLUX outputs for different "target box" top lid (820 hPa and 770 hPa) and horizontal extensions (2°x2° and 3°x3°).*

Basing on these results, we can summarize that STEFLUX showed satisfactory performances for PRS, which are somewhat comparable with the results obtained by Cui et al. (2009) by applying Lagrangian models for detecting SI at the high alpine site Jungfraujoch (Switzerland). STEFLUX performances appeared to decrease moving towards southern latitudes and lower altitudes. However, in the latter case, it must be considered that relatively short time series were available for the assessment.

3.3.5 Scientific highlights

Long-term trend investigation of atmospheric climate-altering and pollutant compounds at CMN

The CNR "O. Vittori" observatory, hosts several programs for long-term observations of climate-altering chemical species, in collaboration with a number of international partners, including: stratospheric ozone-depleting halocarbons, regulated by the Montreal Protocol, non-CO_2 greenhouse gases, included in Kyoto Protocol basket, ozone and non-methane volatile organic compounds (NM-VOC), mineral aerosol and black carbon. These activities are fundamental to analyse long-term trends and to quantify and localize emission sources, highlighting the importance of support long-term observational system programmes. Concerning the stratospheric O_3 depleting substances (ODS, i.e. CFC, HCFCs, halons, CH3CCl3, CCl_4, CH_3Cl, CH_3Br), analysed at CMN since early 2000's, the observed trends confirm the success of Montreal Protocol but at the same time point to the persistence of unaccounted emissions from European regions (especially for CH3CCl3, CCl_4, CH_3Cl, CH_3Br). The four monitored CFCs and halon H-1211 and H-1301 showed negative or levelling-off trends. HCFC-141b and HCFC-142b still show increasing trends but with almost zero or negative acceleration. A decreasing trend is also pointed out for CH_3CCl_3 and CCl_4 but over period 2002-2012, unexpected sources have been observed in Europe for CH_3CCl_3 (south-eastern France, related with landfill and waste disposal and halogen chemical production plants) and CCl_4 (Southern France, Central England, and BE-NE-LUX, where most of industrial scale production of basic organic chemicals are located). CH_3Br measurements showed a negative trend at CMN but an increase of "peak" episodes occurred in 2010–2011, suggesting a massive and

unreported use of stocks (probably in Italy and Spain, where this chemical was used as agricultural fumigant). Non-CO_2 greenhouse gases (HFCs, CH_4 and N_2O) included in Kyoto Protocol show significant increasing trends (see Maione, 2017), while downward tendencies are observed for atmospheric compounds regulated by European air quality directives. In particular, over the period 1996 - 2016, a negative trend (significant at the 99% confidence level) of -0.21 ppb/year was calculated for near-surface O_3. In particular, the largest trend decrease was detected for summer (Cristofanelli et al., 2015). This would reflect the decrease of O_3 precursor emissions within Europe and northern Italy as confirmed by the non-methane volatile organic compound (NM-VOC) observations at CMN (Lo Vullo et al., 2016) which led to reductions in peak summertime O_3 also at continental sites.

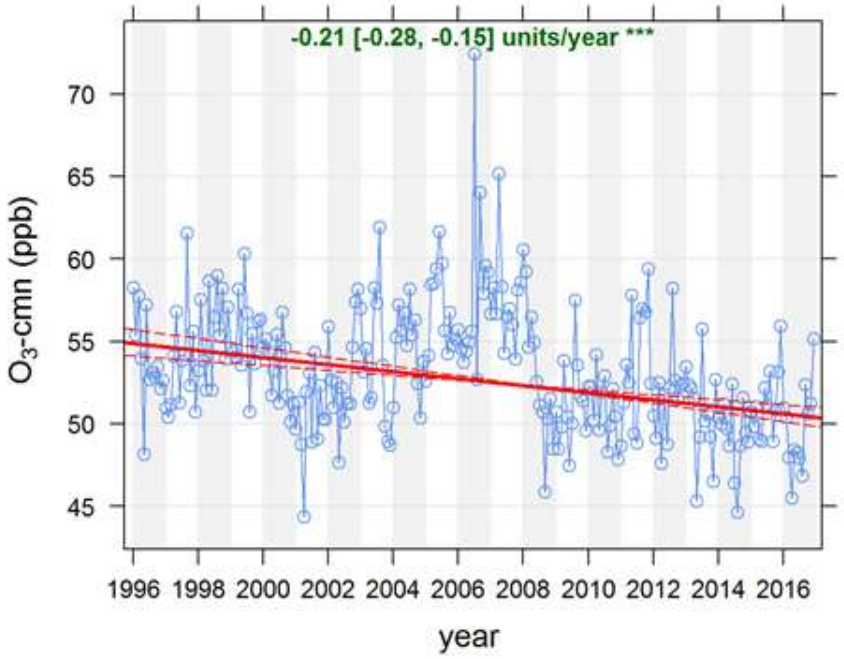

Figure 6. *Time series of de-seasonalised monthly O_3 values at CMN. The results of the trend calculated by the Theil-Sen method is reported by the bold red line together with the 95% confidence interval (dotted red lines). The annual trend value is reported over each plot.*

For the period 2005-2013, Putero and Landi (2017), showed a statistically significant negative trend of -0.17 μg m^{-3} $year^{-1}$ for equivalent black carbon (eqBC), an aerosol produced by the incomplete combustion of fossil fuels and biomass: heating systems, industries, traffic (in particular "Diesel" engines), agricultural and forest fires. Both, O_3 and BC, besides to be atmospheric pollutants play a role as short-lived climate forcers (UNEP & WMO, 2011). This result appears in agreement with independent studies conducted in the Po Valley region (e.g. Bigi and Ghermandi, 2016; Putaud et al., 2014) and showing negative tendencies for the concentration of fine particles and absorbing aerosol, probably linked to European policies for the containment of PM10 concentrations.

Transport of air pollutants to mountain areas

In the framework of NextData, we analysed reactive gases (O_3, CO, NO_x) and aerosol properties (eqBC, σs and particle number concentration) collected at CMN during an experimental campaign

which occurred on summer 2012 (Cristofanelli et al., 2016). The major aim of this experiment was to provide a characterization of the variability of summer atmospheric composition over the central Mediterranean basin, which is considered as a global "hot-spot" for atmospheric pollution and climate change.

The atmospheric tracers have been analyzed as a function of (i) meteorological parameters, (ii) synoptic-scale circulation and (iii) anthropogenic emission source proximity as estimated by O_3/NOx ratio variability. In particular, we identified three O_3/NOx regimes, which tagged the distance of anthropogenic sources: near outflow (23% of hourly data), far-outflow (38% of data) and background (39% of data). The highest levels of anthropogenic pollutants (e.g. O_3, CO, eqBC, accumulation particles) were concomitant with fresh emissions from northern Italy under near-outflow conditions: once injected to the free troposphere, these air-masses, rich in pollutants and climate-forcers (i.e. O_3, eqBC) and soil dust, can be spread over a large region, thus significantly affecting regional climate.

In the framework of NextData, continuous O_3 measurements were implemented at MRG, in the Dolomite mountains. The first year (2017) of continuous observations at MRG, were analyzed to provide first hints about possible transport of air-masses influenced by anthropogenic emissions.

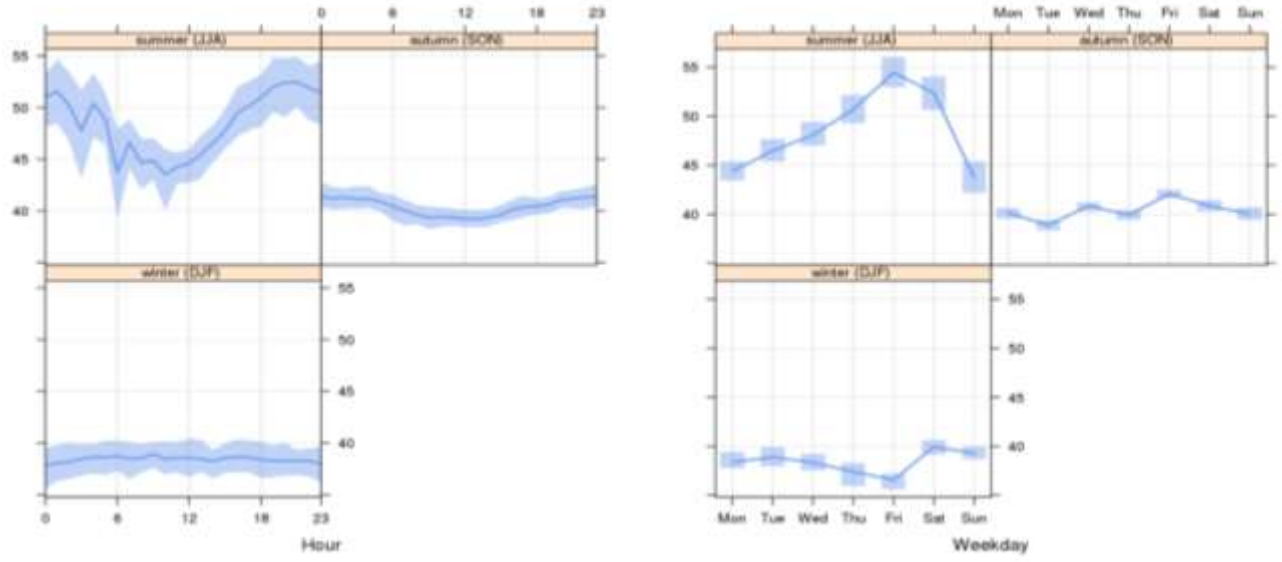

Figure 7. *Averaged variabilities of O_3 (ppb) at MRG during 2017. Left: typical seasonal variabilities. Right: typical weekly variabilities. The shaded area denote the 95% confidence interval. Time is expressed in UTC.*

According to other mountain sites, a diurnal O_3 variability was evident at MRG during summer season, with highest value during evening-night and the lowest during day-time (Figure 7). This "reversal" diurnal variation, can be related to the transport from the PBL of air-masses poorer in O_3, as well as to dry deposition processes occurring along mountain slope during the central part of the day. On the other side, on afternoon-evening, transport of air-masses richer in O_3 produced within the PBL or present in residual layers above the PBL or from the free troposphere (especially during night-time, due to long-range transport) can be considered. It is interesting to note, the occurrence of a significant weekly cycle at MRG during summer, with values increasing during the week. This would suggest the occurrence, during favorable weather conditions, of O_3 build-up due to the impact of anthropogenic emissions. A reverse cycle is observed during winter instead,

pointing towards an influence of anthropogenic emissions (by NO titration) occurring at regional/continental scales even during this season (Gilge et al., 2010).

Example of results about modelling of ozone variability in the Mediterranean central Apennines

In the framework of NextData, O_3 and the meteorological parameters collected at CMP during an experimental campaign carried out on summer 2012 have been analysed. The major aim of this experiment was to characterization O_3 with a stepwise regression model to identify the parameters that controls its variability in the mountain site in Central Italy (Cristofanelli et al., 2013). In Figure 8 are reported the diurnal average of O_3, solar radiation, air pressure, temperature, dewpoint temperature and wind velocity and direction. The meteorological parameters were used to build a linear regression model to describe the O_3 variations using a stepwise technique that iteratively alters the model by adding or removing a predictor variable to maximize the regression coefficients between model and measurements (Biancofiore et al., 2015). Using the stepwise technique, we exclude redundant variable predictors like temperature, wind velocity and direction, and identify solar radiation, pressure and dewpoint temperature as the best set of predictors for O_3. Comparing the diurnal average of the measured and modeled O_3 (left upper panel of Figure 8), the model simulate quite well the diurnal variation with a lightly underestimation of the diurnal peak at around 17:00, and an over estimation at 21:00.

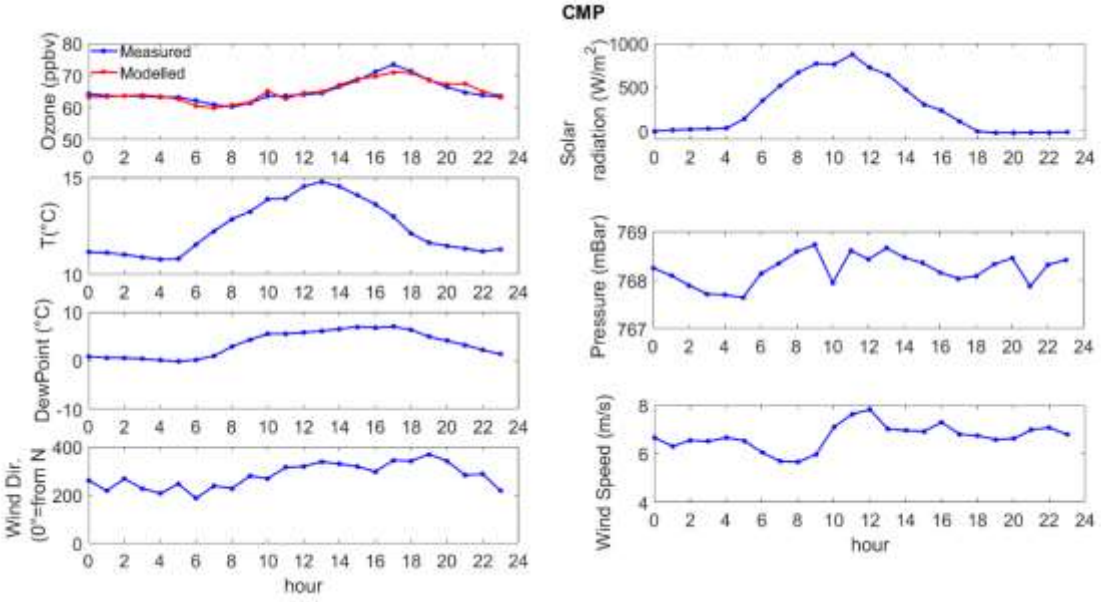

Figure 8. *Diurnal variation of measured and modelled O_3 and observed meteorological parameters at CMP station in August 2012.*

The linear model identified by the stepwise regression is:

*O_3(modelled) = C1*Solar_Radiation(measured) + C2*Air_Pressure(measured) + C3*Dewpoint_Temperature(measured)*

where the coefficient C1, C2 and C3 are reported in table 10, which includes also the statistics parameters of the coefficients that indicate solar radiation and dewpoint temperature with high significance (more than 99%), whereas air pressure with a significance of more than 95%, but less than 99%. These results suggest that O_3 are mainly controlled by solar radiation and an indirect proxy of vertical transport as dewpoint temperature that may indicates intrusion at the observational site of drier air richer of O_3 from higher atmospheric layers. Modelled versus

measured O_3 (here not shown) shows good agreement, with a slope of 0.9, an average bias of about 6 ppbv, R^2 = 0.9 and p-value $<1 \cdot 10^{-9}$. Further tests of the model with hourly data and for a longer period are planned to improve the model constrains, and to better characterize the role of meteorological parameters in the variability of O_3 at CMP.

Model Predictor	**Coefficient**	**Standard error of the coefficient**	**p-value**
Solar Radiation (W/m^2)	0.0065	0.0009	$<1 \cdot 10^{-9}$
Air Pressure (mBar)	2.4569	0.9677	0.0195
Dewpoint Temperature (°C)	1.2781	0.1042	$<1 \cdot 10^{-9}$

Table 10. *Results of the stepwise regression model, including the statistics of the identified coefficients.*

Desert dust and cloud radiative effects in the remote Mediterranean basin

Within NextData, the optical properties of desert dust and their radiative effects in the infrared spectral region have been investigated (Meloni et al., 2018) by using observations performed during the Chemistry-Aerosol Mediterranean Experiment/ Aerosol Direct Radiative Impact on the regional climate in the MEDiterranean region (ChArMEx/ADRIMED) experiment in June-July 2013. This field campaign was carried out at different Mediterranean sites, and in particular at LMP (www.lampedusa.enea.it). Two French aircraft, the ATR42 and the Falcon 20, performed several flights to monitor vertical profiles of atmospheric thermodynamic state, aerosol physical, chemical, and optical properties, and radiation, respectively within and above the dust layers. Onboard the ATR42, the CLIMAT radiometer also measured nadir infrared brightness temperatures (BTs) in three narrowband channels centered at 8.7, 10.6, and 12 µm.

The MODTRAN5 radiative transfer model was fed with observations of the atmospheric vertical structure and composition, in order to simulate the observed radiation quantities (surface broadband longwave and 8-14 µm irradiance, zenith sky BT in the 9.6-11.5 µm interval), and to estimate the infrared aerosol radiative effect (ARF) at the surface, at the top of the atmosphere, and within the atmosphere, as well as the aerosol heating rates (AHR), based on different assumptions on the particles size distribution (AERONET and in situ) and various dust refractive indices from literature (Hess et al., 1998) and from laboratory analyses on dust samples (Di Biagio et al., 2017) collected in different dust source regions (Tunisia, Algeria, Morocco).

The results show that similar longwave irradiances are produced by different combinations of particle size distribution and refractive index, thus not permitting to reduce the uncertainty on the dust refractive index. On the contrary, the integration of in situ radiation measurements at different levels in the atmosphere and in different infrared bands helps constraining the aerosol properties and the radiative effects. The calculated dust radiative effect and heating rates strongly depend on the assumed size distributions and refractive indices (Figure 9).

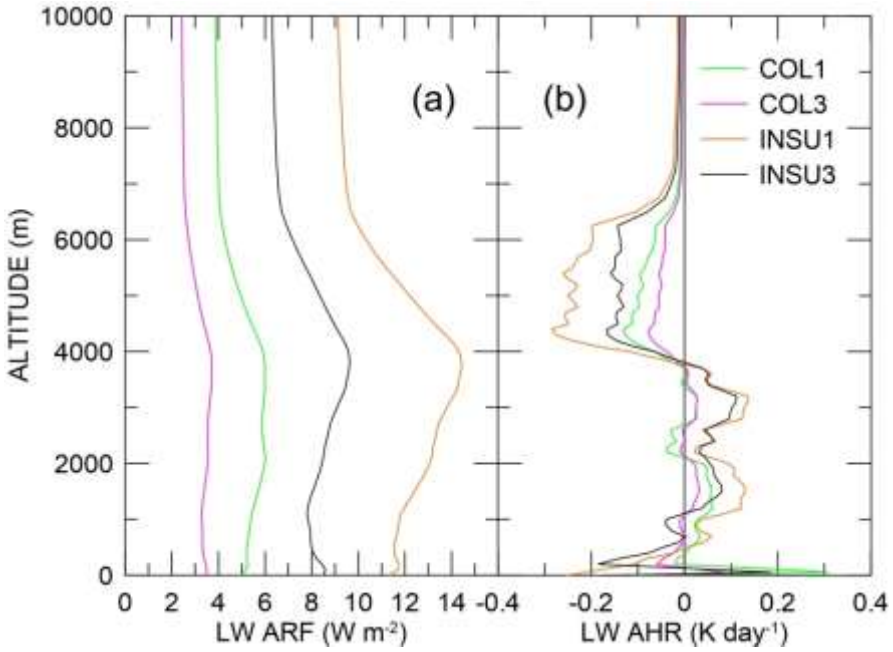

Figure 9. *Longwave (a) ARF and (b) AHR profiles calculated from measurements and MODTRAN simulation on 22 June. The different curves are obtained with various combination of aerosol size distribution and refractive index: COL with the columnar AERONET size distribution, INSU with the size distribution from airborne measurements; the number 1 indicates the literature dust complex refractive index, the number 3 the dust refractive index from the analyses of soil samples on the dust source region.*

The ARF may change by a factor as large as 2.5 at the surface and 2.7 at the top of the atmosphere, depending on the particle size distribution and refractive index, for cases producing a good agreement with observed irradiances.

Thus, the knowledge of the particle size distribution and refractive index is crucial for a correct estimate of the dust radiative effect and heating rate. The experiment also shows that IR effects are important when considering dust aerosols.

Knowledge of photosynthetically active radiation (PAR), reaching the Earth's surface, is essential for the determination of biomass production and for the understanding of terrestrial and marine vegetation physiology. Nevertheless, despite its importance, few direct measurements of PAR are carried out routinely in the World, especially for the diffuse component. As part of NextData activity, a method was developed to derive global (direct+diffuse) and diffuse PAR from observations made with multi filter rotating shadowband radiometers (MFRSRs) at LMP observatory. The method is based on the comparison between MFRSR observations made in the PAR spectral range (4 bands) and a freshly calibrated PAR sensor (Trisolino et al., 2016; 2018). PAR measurements have been carried out at the Station for Climate Observation at Lampedusa since 2004 by means of Li-Cor Li 190 quantum sensors.

The method has been applied to the time series of MFRSR measurements from 2002 to 2016, and the time evolution of global and diffuse PAR have been analyzed (Figure 10). The global PAR presents a maximum in summer, while the behavior of the diffuse PAR is more complex, with two maxima in April and June, due to the role of atmospheric aerosols.

With the aim to quantitatively assess the impact of clouds on the PAR, the global and diffuse cloud-free PAR have been derived by first selecting cloud-free periods and then by fitting the

cloud-free time series with a simple oscillatory function, shown in Figure 10 for both global and diffuse irradiance.

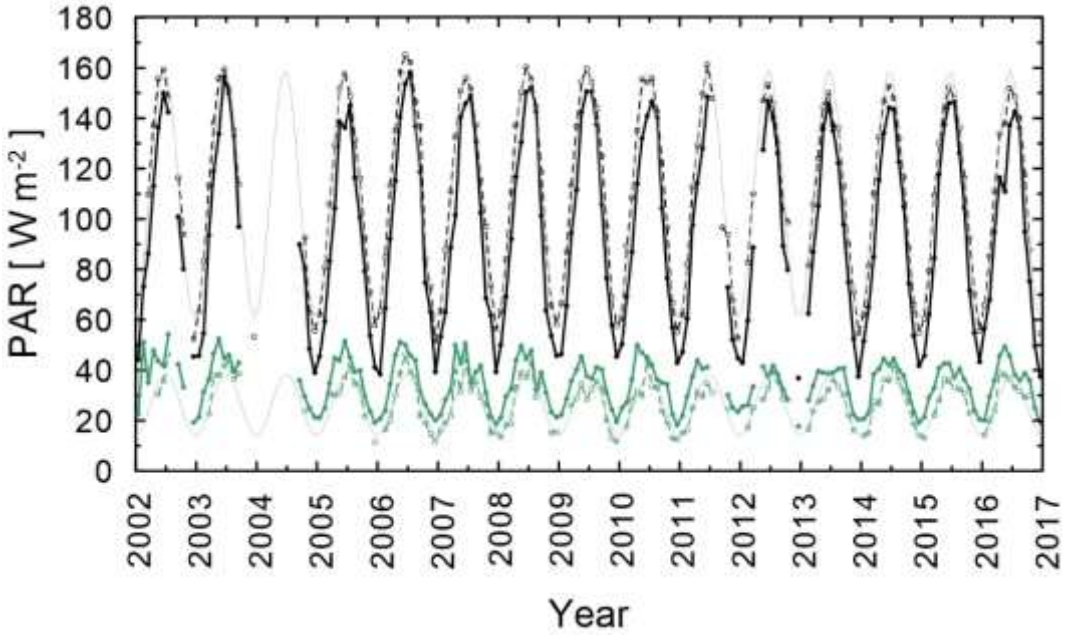

Figure 10. *Time series of monthly mean global (black curve) and diffuse (green curve) PAR for cloud-free (dashed lines) and all sky conditions (continuous lines). Fitting curves (see text) are shown by thin lines for the cloud-free time series.*

The cloud radiative effect (CRE) has been calculated for the global and diffuse PAR: they show a similar behavior, but with opposite sign, i.e. negative for the global and positive for the diffuse PAR. The long-term average CRE is -14.7 Wm^{-2} for global PAR and +8.1 Wm^{-2} for diffuse PAR.
The dependence of the CRE on the cloud properties has been studied based on the information derived from the MODIS sensor onboard Aqua. Level 3 monthly mean cloud optical thickness (COT), cloud fraction (CF), and cloud top pressure (CTP) determined from July 2002 to December 2016 over a region 2°x2° around Lampedusa have been used. The results show that about 77% of the global PAR interannual variability is associated with the cloud variability in winter and 31% in summer. The cloud influence on diffuse PAR is more difficult to disentangle, due to the stronger dependency on cloud properties.

Acknowledgments

CNR-ISAC gratefully acknowledges the Italian Air Force, CAMM Mt. Cimone for their active logistic and technical support at Mt. Cimone.
Alcide di Sarra acknowledges the activities by F. Anello, C. Bommarito, T. Di Iorio and F. Monteleone, concerning the execution of observations and data analysis at LMP observatories.
The research activity on going at Plateau Rosa monitoring station have been primarily financed by the Research Fund for the Italian Electrical System under the Contract Agreement between RSE SpA and the Italian Ministry of Economic Development - General Directorate for Nuclear Energy, Renewable Energy and Energy Efficiency, stipulated on July 29, 2009, in compliance with the Decree of November 11, 2012.

References

Anderson T. L., Ogren J. A., 1998. Determining Aerosol Radiative Properties Using the TSI 3563 Integrating Nephelometer, Aerosol Science and Technology, 29(1):57-69, DOI: 10.1080/02786829808965551.

Biancofiore F., Verdecchia M., Di Carlo P., Tomassetti B., Aruffo E., Busilacchio M., Bianco S., Di Tommaso S., Colangeli C., 2015. Analysis of surface ozone using a recurrent neural network, Science of the Total Environment, 514:379–387.

Bigi A., Ghermandi G., 2014. Long-term trend and variability of atmospheric PM10 concentration in the Po Valley, Atmospheric Chemistry and Physics, 14:4895-4907.

Bonasoni P., Stohl A., Cristofanelli P., Calzolari F., Colombo T., Evangelisti F., 2000. Background ozone variations at Mt. Cimone Station. Atmospheric Environment, 34:5183–5189.

Carslaw D.C., Ropkins K., 2012. Openair — an R package for air quality data analysis. Environmental Modelling & Software, 27-28:52–61.

Cinnirella S., D'Amore F., Bencardino M., Sprovieri F., Pirrone N., 2014. The GMOS cyber(e)-infrastructure: advanced services for supporting science and policy. Environmental Science and Pollution Research, 21(6):4193-4208. doi: 10.1007/s11356-013-2308-3.

Collaud Coen M., Weingartner E., Schaub D., Hueglin C., Corrigan C., Henning S., Schwikowski M., Baltensperger U., 2004. Saharan dust events at the Jungfraujoch: detection by wavelength dependence of the single scattering albedo and first climatology analysis. Atmos. Chem. Phys., 4:2465–2480.

Colombo T., Santaguida R., Capasso A., Calzolari F., Evangelisti F., Bonasomi P., 2000. Biospheric influence on carbon dioxide measurements in Italy. Atmospheric Environment, 34:4963-4969.

Cristofanelli P., Di Carlo P., D' Altorio A., Salisburgo C., Tuccella P., Biancofiore F., Stocchi P., Verza G. P., Landi T. C., Marinoni A., Calzolari F., Duchi R., Bonasoni P., 2013. Analysis of Summer Ozone Observations at a High Mountain Site in Central Italy (Campo Imperatore, 2388 m a.s.l.), Pure Appl. Geophys, 170:1985-1999.

Cristofanelli P., Landi T.C., Calzolari F., Duchi R., Marinoni A., Rinaldi M., Bonasoni P., 2016. Summer atmospheric composition over the Mediterranean basin: Investigation on transport processes and pollutant export to the free troposphere by observations at the WMO/GAW Mt. Cimone global station (Italy, 2165 m a.s.l.). Atmospheric Environment, 141.

Cristofanelli P., Busetto M., Calzolari F., Ammoscato I., Gullì D., Dinoi A., Calidonna C.R., Contini D., Sferlazzo D., Di Iorio T., Piacentino S., Marinoni A., Maione M., Bonasoni P., 2017. Investigation of reactive gases and methane variability in the coastal boundary layer of the central Mediterranean basin. Elem Sci Anth, 5: 12, DOI: https://doi.org/10.1525/elementa.216.

Cristofanelli P., Brattich E., Decesari S., Land T. C., Maione M., Putero D., Tositti L., Bonasoni P., 2018. The Italian Mt. Cimone WMO/GAW Global Station (2165 m a.s.l.), High-Mountain Atmospheric Research, SpringerBriefs in Meteorology, doi: 10.1007/978-3-319-61127-3.

Cui J., Sprenger M., Staehelin J., Siegrist A., Kunz M., Henne S. and Steinbacher M., 2009. Impact of stratospheric intrusions and intercontinental transport on ozone at Jungfraujoch in 2005: comparison and validation of two Lagrangian approaches, Atmos. Chem. Phys., 9:3371–3383, doi:10.5194/acp-9-3371-2009.

Decesari S., 2017. Aerosol Chemical Composition at the Mt. Cimone WMO/GAW Global Station. In: High-Mountain Atmospheric Research - The Italian Mt. Cimone WMO/GAW Global Station (2165 m a.s.l.). Amsterdam: Springer.

Di Biagio C., Formenti P., Balkanski Y., Caponi L., Cazaunau M., Pangui E., Journet E., Nowak S., Caquineau S., Andreae M. O., Kandler K., Saeed T., Piketh S., Seibert D., Williams E., and Doussin J. F., 2017. Global scale variability of the mineral dust longwave refractive index: a new dataset of in situ measurements for climate modelling and remote sensing, Atmos. Chem. Phys., 17:1901–1929, doi:10.5194/acp-17-1901-2017.

Duchi R., Cristofanelli P., Landi T. C., Arduini J., Bonafè U., Bourcier L., Busetto M., Calzolari F., Marinoni A., Putero D., Bonasoni P., 2016. Long-term (2002–2012) invesrigation of Saharan dust transport events at Mt. Cimone GAW global station, Italy (2165 m a.s.l.). Elementa, 4, 000085, doi:10.12952/journal.elementa.000085.

GAW, 2011. Expert Workshop on Global Long-term Measurements of Nitrogen Oxides and Recommendations for GAW Nitrogen Oxides Network, Hohenpeissenberg Meteorological Observatory (Germany, October 2009).

GAW Report No. 192. Guidelines for the Measurement of Atmospheric Carbon Monoxide.

GAW Report No. 200. WMO/GAW Standard Operation Procedures for in-situ measurements of aerosol mass concentration, light scattering and light absorption.

GAW Report No. 209. Guidelines for Continuous Measurements of Ozone in the Troposphere.

GAW Report No. 213. 17th WMO/IAEA meeting on Carbon Dioxide, other greenhouse gases and related tracers measurements techniques (GGMT-2013).

GAW Report No. 227. WMO/GAW Aerosol Measurement procedures, Guidelines and Recommendations, 2nd Edition, 2016.

Gilge S., Pass-Duelmer C., Roher F., Steinbacher M., Fjaeraa A. M., Lageler F., Walden J., 2014. Deliverable D4.10: Standardized operating procedures (SOPs) for NO_{xy} measurements. http://fp7.actris.eu/Portals/97/deliverables/PU/WP4_D4.10_M42.pdf.

Finnish Meteorological Institute, ACTRIS Stakeholder Handbook, 2017. ISBN 978-952-336-049-5 (pdf version), 2017.

Hazan L., Tarniewicz J., Ramonet M., Laurent O., Abbaris A., 2016. Automatic processing of atmospheric CO_2 and CH*4* mole fractions at the ICOS Atmosphere Thematic Centre, Atmos. Meas. Tech., 9:4719-4736, https://doi.org/10.5194/amt-9-4719-2016.

Hess M., Koepke P. and Schult I., 1998. Optical properties of aerosols and clouds: the software package OPAC, Bull. Amer. Meteorol. Soc., 79:831-844, 1998, https://doi.org/10.1175/1520-0477 (1998)079<0831:OPOAAC>2.0.CO;2.

Huang S., Wang Y., Xie Y., Zhao P., Lüers J., 2016. OutlierFlag: a tool for scientific data quality control by outlier data flagging, J. Open Res. Softw., 4, e20, doi:10.5334/jors.90.

Lo Vullo E.L., Furlani F., Arduini J., Giostra U., Cristofanelli P., Williams M. L., Maione M., 2016. Non-Methane Volatile Organic Compounds in the background atmospheres of a southern European mountain site (Mt. Cimone, Italy): an-nual and seasonal variability. Aerosol and Air Quality Research, vol 16:581–592.

Maione M., 2017. Non-CO_2 Greenhouse Gases. In: High-Mountain Atmospheric Research - The Italian Mt. Cimone WMO/GAW Global Station (2165 m a.s.l.). Amsterdam: Springer.

Meloni D., di Sarra A., Brogniez G., Denjean C., De Silvestri L., Di Iorio T., Formenti P., Gómez-Amo J. L., Gröbner J., Kouremeti N., Liuzzi G., Mallet M., Pace G., and Sferlazzo D. M., 2018. Determining the infrared radiative effects of Saharan dust: a radiative transfer modelling study based on vertically resolved measurements at Lampedusa, Atmos. Chem. Phys., 18:4377–4401, 2018. doi: 10.5194/acp-18-4377-2018.

Müller T., Laborde M., Kassell G. and Wiedensohler A., 2011. Design and performance of a three-wavelength LED-based total scatter and backscatter integrating nephelometer, Atmos. Meas. Tech., 4:1291-1303, https://doi.org/10.5194/amt-4-1291-2011, 2011.

Petzold A., Schönlinner M., 2004. Multi-angle absorption photometry—a new method for the measurement of aerosol light absorption and atmospheric black carbon. Journal of Aerosol Science, 35 (4):421-441.

Putaud J.P., Van Dingenen R., Dell'Acqua A., Raes F., Matta E., Decesari S., Facchini M. C. and Fuzzi S., 2004. Size-segregated aerosol mass closure and chemical composition in Monte Cimone (I) during MINATROC. Atmospheric Chemistry and Physics, vol 4:889-902.

Putero D., Cristofanelli P., Sprenger M., Škerlak B., Tositti L. and Bonasoni P., 2016. STEFLUX, a tool for investigating stratospheric intrusions: application to two WMO/GAW global stations. Atmos. Chem. Phys., 16:14203–14217.

Putero D., Landi T., 2017. Statistical Analysis of Essential Climate Variables (ECVs) at Mt. Cimone. In: High-Mountain Atmospheric Research - The Italian Mt. Cimone WMO/GAW Global Station (2165 m a.s.l.). Amsterdam: Springer.

R Development Core Team, 2015. R: A Language and Environment for Statistical Computing. R Foundation for Statistical Computing, Vienna.

Schultz M. G., Akimoto H., Bottenheim J. Buchmann B., Galbally I. E., Gilge S., Helmig D., Koide H., Lewis A. C., Novelli P. C., Plass- Dülmer C., Ryerson T. B., Steinbacher M., Steinbrecher R., Tarasova O., Tørseth K., Thouret V., Zellweger C., 2015. The Global Atmosphere Watch reactive gases measurement network. Elem Sci Anth. doi: 10.12952/journal.elementa.000067.

Škerlak B., Sprenger M. and Wernli H., 2014. A global climatology of stratosphere-to-troposphere exchange using the ERA-Interim data set from 1979 to 2011. Atmos. Chem. Phys., 14.

Sprovieri F., Pirrone N., Bencardino M., D'Amore F., Carbone F., Cinnirella S., Mannarino V., Landis M., Ebinghaus R., Weigelt A., Brunke E. G., Labuschagne C., Martin L., Munthe J., Wängberg I., Artaxo P., Morais F., Barbosa H. D. M. J., Brito J., Cairns W., Barbante C., Diéguez M. D. C., Garcia P. E., Dommergue A., Angot H., Magand O., Skov H., Horvat M., Kotnik J., Read K. A., Neves L. M., Gawlik B. M., Sena F., Mashyanov N., Obolkin V., Wip D., Feng X. B., Zhang H., Fu X., Ramachandran R., Cossa D., Knoery J., Marusczak N., Nerentorp M. and Norstrom C., 2016. Atmospheric mercury concentrations observed at ground-based monitoring sites globally distributed in the framework of the GMOS network. Atmospheric Chemistry and Physics, 16(18):11915-11935.

Stein A.F. and Ngna F., 2015. NOAA's HYSPLIT Atmospheric Transport and Dispersion Modeling System. doi.org/10.1175/BAMS-D-14-00110.1.

Steinbacher. M., Zellweger C., Schwarzenbach B., Bugmann S., Buchmann B., Ordó$ez C., Prevot A. S. H. and Hueglin C., 2007. Nitrogen oxide measurements at rural sites in Switzerland: Bias of

conventional measurement techniques, J. Geophys. Res., 112, D11307, doi:10.1029/2006JD007971.

Thornes J. E. and Stephenson D. B., 2001. How to judge the quality and value of weather forecast products. Meteorol. Appl., 8:307–314.

Trickl T., Feldmann H.-J., Kanter H.-J., Scheel H. E., Sprenger M., Stohl A. and Wernli H., 2010. Forecasted deep stratospheric intrusions over Central Europe: case studies and climatologies, Atmos. Chem. Phys., 10:499–524, doi:10.5194/acp-10-499-2010.

Trisolino P., di Sarra A., Meloni D. and Pace G., 2016. Determination of global and diffuse photosynthetically active radiation from a multifilter shadowband radiometer, Appl. Optics, 55:8280– 8286.

Trisolino. P., di Sarra A., Anello F., Bommarito C., Di Iorio T., Meloni D., Monteleone F., Pace G., Piacentino S. and Sferlazzo D., 2018. A long-term time series of global and diffuse photosynthetically active radiation in the Mediterranean: interannual variability and cloud effects, Atmos. Chem. Phys., 18, 7985-8000, https://doi.org/10.5194/acp-18-7985-2018, 2018.

UNEP & WMO, 2011. Integrated Assessment of Black Carbon and Tropospheric Ozone.

Wiedensohler A., Birmili W., Nowak A., Sonntag A., Weinhold K., Merkel M., Wehner B., Tuch T., Pfeifer S., Fiebig M., Fjäraa A. M., Asmi E., Sellegri K., Depuy R., Venzac H., Villani P., Laj P., Aalto P., Ogren J. A., Swietlicki E., Williams P., Roldin P., Quincey P., Hüglin C., Fierz-Schmidhauser R., Gysel M., Weingartner E., Riccobono F., Santos S., Grüning C., Faloon K., Beddows D., Harrison R., Monahan C., Jennings S. G., O'Dowd C. D., Marinoni A., Horn H.-G., Keck L., Jiang J., Scheckman J., McMurry P. H., Deng Z., Zhao C. S., Moerman M., Henzing B., de Leeuw G., Löschau G. and Bastian S., 2012. Mobility particle size spectrometers: harmonization of technical standards and data structure to facilitate high quality long-term observations of atmospheric particle number size distributions, Atmos. Meas. Tech., 5, 657-685, https://doi.org/10.5194/amt-5-657-2012, 2012.

Wilks D. S., 2006. Statistical methods in the atmospheric sciences: an introduction, 2nd Edn., Academic press.

World Meteorological Organization, GCOS Implementation Plan 2016 (2016).

World Meteorological Organization, WMO Global Atmosphere Watch (GAW) Implementation Plan: 2016-2023 (2017) GAW Report n. 228.